0013-7227/08/$15.00/0
Printed in U.S.A.

Endocrinology 149(7):3461–3469

doi: 10.1210/en.2007-1692

Autoimmune Hypophysitis of SJL Mice: Clinical Insights from a New Animal Model

Shey-Cherng Tzou, Isabella Lupi, Melissa Landek, Angelika Gutenberg, Ywh-Min Tzou, Hiroaki Kimura, Giovanni Pinna, Noel R. Rose, and Patrizio Caturegli

Department of Pathology (S.-C.T., I.L., M.L., A.G., H.K., N.R.R., P.C.), The Johns Hopkins University, School of Medicine, and Feinstone Department of Molecular Microbiology and Immunology (N.R.R., P.C.), The Johns Hopkins, Bloomberg School of Public Health, Baltimore, Maryland 21205; Department of Endocrinology and Metabolism (I.L.), University of Pisa, 43-56126 Pisa, Italy; Department of Neurosurgery (A.G.), Georg-August-University Goettingen, 37077 Goettingen, Germany; Department of Nutrition & Food Science (Y.-M.T.), Auburn University, Auburn, Alabama 36849; and Endocrinology Unit (G.P.), Department of Medical Science "M. Aresu," Azienda Ospedaliera, University of Cagliari, 09042 Monserrato (CA), Italy

Autoimmune hypophysitis (AH) is a rare but increasingly recognized disease of the pituitary gland. Its autoantigens are unknown, and the management is difficult because it is often misdiagnosed as a nonsecreting adenoma. By immunizing female SJL/J mice with mouse pituitary extracts, we established a new mouse model of experimental AH. Immunized mice developed severe lymphocytic infiltration in the anterior pituitary that closely mimicked the human pathology. In the early phase of experimental AH, the pituitary enlarged, consistent with the compression symptoms reported by hypophysitis patients at presentation. In the florid phase, adrenal insufficiency and pituitary antibodies developed, in strong correlation with the pituitary pathology. In the late phase, hypothyroidism ensued, and the pituitary gland became atrophic. Using immune sera as probes in a two-dimensional immunoblotting screen followed by mass spectrometry, we identified several proteins that could function as pituitary autoantigens. These findings provide new insights into the pathogenesis of AH, and establish a platform for developing novel diagnostic biomarkers and therapeutics. (*Endocrinology* 149: 3461–3469, 2008)

AUTOIMMUNE hypophysitis (AH), also known as lymphocytic hypophysitis, is an increasingly recognized disease of the pituitary gland (1) that belongs to the group of nonhormone-secreting pituitary masses (2). AH affects more commonly women, often in association with pregnancy, and typically presents with two types of symptoms: those due to compression of the structures surrounding the pituitary, such as headache (meninges), visual-field defect (optic chiasm), and diplopia (oculomotor nerves); and those of hypopituitarism (3). However, these symptoms are not specific for AH but typical of all pituitary masses, such as the more common pituitary adenoma. Even cranial magnetic resonance imaging cannot distinguish with certainty AH from the other nonsecreting pituitary masses (1). The distinction is critical for the affected patients because AH can often be managed with medical therapy, whereas the other pituitary masses typically require surgical resection. Unfortunately, many AH patients are still misdiagnosed and undergo unnecessary transsphenoidal surgery (4).

AH incidence is likely underestimated because compression symptoms may be mild and hypopituitarism subclinical. A surprisingly high incidence of AH has been recently reported in patients with melanoma (5) or renal cell cancer (6) who received cytotoxic T-lymphocyte-associated antigen-4 blockade. For example, 5% of patients with advanced melanoma treated with a vaccine for the gp100 melanoma-associated antigen and an antibody to block cytotoxic T-lymphocyte-associated antigen-4 developed AH. AH has also been reported in hepatitis patients treated with interferon α (7, 8), suggesting that it might occur (albeit unnoticed) in settings aimed to boost immune responsiveness.

AH antigen(s) has remained unknown, despite the fact that the disease was first reported in 1962. Five candidates have been proposed [GH (9), α-enolase (10), pituitary gland specific factors 1 and 2 (11), and secretogranin 2 (12)], but they have not been validated in human or animal studies. This uncertainty has hampered the development of antibody based clinical tests that could be used in the differential diagnosis of pituitary masses.

In addition, a mouse model that faithfully replicates the pathology of human AH has not been developed. In 1981, Onodera *et al*. (13) infected SJL mice with reovirus type 1, and noted diabetes, gastritis, and growth retardation. They showed viral particles within GH-producing cells and antibodies against anterior pituitary cells that could be preabsorbed with rat GH. They also described areas of coagulative necrosis and mononuclear cell infiltration in the anterior pituitary, although the pituitary gland appears normal (no architectural disruption or infiltration) in the immunofluorescence image used to show antibody reactivity. In 2002, de Jersey *et al*. (14) created transgenic mice that expressed specifically in GH-producing cells the nucleoprotein of influ-

First Published Online April 3, 2008

Abbreviations: AH, Autoimmune hypophysitis; AU, arbitrary unit; CFA, complete Freund's adjuvant; CI, confidence interval; EAH, experimental autoimmune hypophysitis; IPG strip, immobilized pH 3–10 gradient strip; PC2, prohormone convertase 2.

***Endocrinology* is published monthly by The Endocrine Society (http://www.endo-society.org), the foremost professional society serving the endocrine community.**

enza A virus (strain A/NT/60/1968). This protein contains an epitope (366–374) recognized by CD8 T cells in a H-2D^b-restricted fashion. When the authors' transgenic mice were crossed to T-cell receptor transgenics specific for the influenza nucleoprotein epitope, the double transgenics developed marked growth retardation. Pituitary histology showed numerous apoptotic bodies and destruction of the GH-producing cells, with scattered infiltrates of CD8 T cells in the anterior pituitary, not reminiscent, however, of the pathology seen in human AH.

This paper reports the first mouse model that closely mimics human AH, and its use in elucidating disease pathogenesis and discovering pituitary autoantigen(s).

Materials and Methods

Mice

The study was performed in three stages and used a total of 514 mice: 462 immunized, 47 nonimmunized, and five recipients of adoptively transferred splenocytes. Of the 462 immunized mice, 367 received proteins extracted from mouse pituitary glands emulsified in complete Freund's adjuvant (CFA), 49 proteins from mouse pituitary cell lines in CFA, 20 recombinant prohormone convertase 2 (PC2) in CFA, 15 control placental proteins in CFA, and 11 just CFA.

The first stage of the study used 146 mice and was designed to identify the mouse strain(s) susceptible to experimental autoimmune hypophysitis (EAH), in view of the known effects of the major histocompatibility complex and sex on autoimmune diseases. Six inbred strains, all purchased from the Jackson Laboratory (Bar Harbor, ME) and first used when 7–8 wk old, were studied: A/J (H-2^a, 15 females and 15 males); Balb/cJ (H-2^d, 15 females and 10 males); C57BL/6J (H-2^b, 15 females and 15 males); CBA/J (H-2^k, 15 females and 10 males); FVB/NJ (H-2^q,10 females); and SJL/J (H-2^s, 17 females and nine males).

The second stage used 344 SJL/J female mice and was designed to select the optimal immunogen dose, characterize the pituitary infiltrate by flow cytometry, demonstrate the transmissibility of disease upon splenocyte transfer, and define the evolution of EAH based on pituitary histopathology, antibodies, and function.

The third stage used 24 SJL/J female mice and tested recombinant PC2, a candidate pituitary autoantigen discovered in the second stage for its ability to induce EAH.

All experiments were conducted in accordance with the standards established by the U.S. Animal Welfare Acts, set forth in the National Institutes of Health guidelines and Policy and Procedures Manual of the Johns Hopkins University Animal Care and Use Committee.

Immunogens

Whole pituitary glands were collected from mice of mixed strains and sexes made available by the Johns Hopkins animal care facility, and stored at −80 C until use. Glands were disrupted with a Polytron homogenizer in PBS (pH 7.4), supplemented with protease inhibitors (Roche Applied Sciences, Indianapolis, IN) to prepare the pituitary whole extract. For each protein extraction, we used about 400 pituitary glands (~780 mg total weight) in 4 ml PBS that yielded around 100-mg proteins. The pituitary whole extract was quantified by a bicinchoninic acid assay (Pierce, Rockford, IL), adjusted to 20 mg/ml, and used directly for immunization or further fractionated. In the latter case, the pituitary whole extract was centrifuged at low speed (1,000 × *g* for 10 min at 4 C) to pellet the nuclear fraction, and then at high speed (100,000 × *g* for 1 h at 4 C) to separate membranes from cytosol. The cytosolic fraction (corresponding to the supernatant) was adjusted to 2, 6, 8, or 10 mg/ml, and used for immunization. The membrane fraction (the ultracentrifugation pellet) was washed and resuspended in PBS/protease inhibitors at 6 or 8 mg/ml.

Mouse pituitary cell lines were αT1–1 (a precursor of gonadotrophs and thyrotrophs expressing the common α-subunit, n = 5 mice), αT3–1 (an immature gonadotroph cell line, n = 5 mice), TαT-1 (a thyrotroph cell line, n = 5 mice), LβT2 (a gonadotroph cell line, n = 5 mice), GHFT5–1 (a precursor of somatotrophs and lactotrophs, n = 5 mice), and AtT-20 (a corticotroph cell line, n = 24 mice). With the exception of AtT-20, which was purchased from the American Type Culture Collection (Manassas, VA), all of the other cell lines were a kind gift of Dr. Pamela Mellon (University of California San Diego, San Diego, CA). Cells were cultured in the recommended medium, harvested, and sonicated to prepare a total lysate. Cell line proteins were quantified and adjusted to 20 mg/ml.

Mouse recombinant PC2 produced in Chinese hamster ovary cells (15) was kindly provided by Dr. Iris Lindberg (University of Maryland, Baltimore, Baltimore, MD) for the initial immunizations and used at a concentration of 1 mg/ml. PC2 was also produced in our laboratory via a bacterial expression system, and used at a concentration of 1, 2, or 6 mg/ml. See supplemental Fig. 3, which is published on The Endocrine Society's Journals Online web site at http://endo.endojournals.org, and supplemental information for details of cloning, production, and purification.

EAH induction protocols

All proteins were emulsified 1:1 in CFA (which contained 5 mg/ml heat-killed *Mycobacterium tuberculosis*, strain H37a, from BD Diagnostic Systems, Sparks, MD), and injected sc on d 0 in a volume of 100 μl (50 μl in the dorsal hind leg region and 50 μl in the contralateral inguinal region). Protein emulsions were injected again on d 7 in the opposite sites. Mice were killed most commonly 28 d after the first immunization, but also on d 10, 14, 21, 28, 35, 56, 84, 112, 140, 252, or 370.

Adoptive transfer of T lymphocytes

To prove that EAH is a cell-mediated autoimmune disease, single-cell suspensions were prepared from the spleens of four SJL/J mice killed 28 d after immunization with pituitary whole extract. Lymphocytes were cultured and expanded in 75-cm^3 flasks in RPMI-10 medium, containing 200 μg/ml mouse pituitary proteins. After 7 d, the nonadherent cells (mainly T lymphocytes) were collected, washed, and resuspended in sterile saline at a concentration of 2×10^8 cells per ml. T lymphocytes were injected into five naive female SJL/J mice via the tail vein (of 2×10^7 cells per mouse). Two weeks after the adoptive transfer, recipients were killed to collect pituitary, thyroid, and pancreas for histopathology.

Pituitary histopathology

To assess the presence and extent of mononuclear infiltration within the pituitary, glands from all 462 mice (the 514 total minus the 52 mice used for pituitary flow cytometry and, thus, without histopathology) were dissected, fixed overnight in Beckstead's fixative, processed, and embedded in paraffin. At least five nonconsecutive sections (one every 10) were cut, stained by hematoxylin and eosin, and analyzed with a digital microscope as described (16) to quantify the mononuclear infiltration of the pituitary gland. EAH was defined histopathologically as a mononuclear infiltration in the pituitary gland greater than 2% of the total anterior pituitary area; mice with such a degree of pituitary infiltration were considered the incidence cases. To assess the extent and evolution of pituitary fibrosis, a subset of 20 pituitaries (15 immunized and five CFA controls), representative of all postimmunization endpoints, were also colored by the Masson's trichrome method, which stains collagen fibers blue, nuclei black, and cytoplasm red. To confirm the organ specificity of the pituitary disease, thyroid gland and pancreas were also collected at the time mice were killed.

Pituitary immunohistochemistry

To analyze the distribution and type of hematopoietic cells infiltrating the pituitary, immunohistochemistry was performed on deparaffinized and rehydrated sections as previously described (17), using the following primary antibodies: B220, CD3, CD11c, CD45 (BD Biosciences, San Jose, VA), and F4/80 (AbD Serotec, Raleigh, NC). Sections were chosen from nine stage 2 mice (five immunized and four controls) and from all stage 3 mice.

Pituitary flow cytometry

To analyze the type, abundance, and activation state of hematopoietic cells infiltrating the pituitary, we studied 52 glands: 22 dissected from

d-28 immunized mice, and 30 nonimmunized controls. For each experiment, five to seven pituitaries were pooled, minced into small pieces (~1 mm^3), and digested for 30 min at 37 C in DMEM (Invitrogen Corp., Carlsbad, CA) containing collagenase II (0.2% wt/vol, from Sigma-Aldrich, St. Louis, MO). Pituitary cells from the digestion were passed through a 70-μm strainer (BD Biosciences), washed, and resuspended in PBS, 1% BSA, 2 mM EDTA, and 0.02% sodium azide at a concentration of 10^7 per ml. Cells were then processed as previously described (16) and stained with fluorochrome-conjugated antibodies (all from BD Biosciences, except when indicated) recognizing the following markers: B220, CD3, CD4, CD8, CD11b, CD44, CD45, CD49b (a pan NK cell marker, clone DX5, from eBioscience, San Diego, CA), and CD69. Cells were then analyzed by FACSCalibur cytometer using CellQuest software (BD Biosciences), gating first on the forward-side scatter to exclude aggregates and dead cells, and then on the CD45-side scatter to identify the hematopoietic cells.

Pituitary antibodies by ELISA

To monitor the humoral immune response against pituitary proteins after immunization, sera were collected before (d 0) and several days after the first immunization (d 7, 10, 14, 21, 28, 35, 56, 84, 112, 140, 200, 252, and 370). Sera were serially diluted in PBS and incubated overnight in Immunolon2 ELISA plates (Dynex Technologies, Chantilly, VA) precoated with mouse pituitary cytosolic proteins (625 ng/well). After washing, IgG and IgM recognizing pituitary antigens were detected using a secondary antibody, conjugated to alkaline phosphatase, and directed against mouse G and M heavy chains (Jackson ImmunoResearch Laboratories, West Grove, PA). Color development was measured at 405 nm using the Emax microplate reader (Molecular Devices, Sunnyvale, CA). Each plate included a homemade standard curve, made by diluting a pool of d-28 post-immunization sera 1:100, 1:400, 1:1,600, 1:6,400, and 1:25,600 in PBS. A value of 5120 arbitrary units (AU) per microliter was assigned to the most concentrated standard (the 1:100 dilution), and corresponding values of 1280, 320, 80, and 20 to the other four standards. This curve allowed us to compare results among plates, expressing results in AU/μl rather than in OD. Preimmune (d 0) sera were used to calculate the normal reference range for SJL/J female mice. Sera were tested in triplicates; sera with a coefficient of variation greater than 20% were excluded. The average coefficient of variation was 6.3%. Intraassay variability was evaluated by measuring the same sera several times during the same assay procedure, and amounted to 4.9 $\pm$ 0.7%. Interassay variability was evaluated by measuring the same sera during different assay procedures, and amounted to 8.6 $\pm$ 1.2%.

Pituitary hormone function

To study pituitary function after immunization, we initially attempted to measure anterior pituitary hormones but failed because the immunization protocol also induced antibodies against these hormones, thus markedly interfering with the assay performance. Therefore, we opted for measuring two key target hormones produced in response to pituitary control, using commercially available RIAs: total T_4 (Diasorin Inc., Stillwater, MN); corticosterone (Diagnostic Systems Laboratories, Webster, TX); and IGF-I (Diagnostic Systems Laboratories). Assay standards and controls were run in duplicate, experimental samples in singlicate and undiluted. Preimmune (d 0) sera were used to calculate the normal reference range for SJL/J female mice.

Identification of candidate pituitary autoantigens by two-dimensional gel electrophoresis, immunoblotting, and mass spectrometry

Pituitary proteins (cytosolic or membrane fractions) were precipitated with 10% trichloroacetic acid/acetone, and redissolved in 7 M urea, 2 M thiourea, 4% 3-[(3-cholamidopropyl)dimethyl ammonio]-1-propanesulfonate, and 30 mM Tris-HCl (pH 8.8). Proteins (250 μg) were initially loaded onto 7-cm long, immobilized pH 3–10 gradient strips (IPG strips) (GE Healthcare, Piscataway, NJ) to identify the most resolving isoelectric point for candidate autoantigens, which was later found to fall between five and seven. Proteins were then loaded onto 24-cm long, pH 4–7 IPG strips, to increase further the resolution of candidate autoantigens in isoelectric focusing buffer (8 M urea, 4% 3-[(3-cholamidopropyl)dimethyl ammonio]-1-propanesulfonate, 0.2% dithiothreitol, 1.5% IPG buffer, 0.002% bromophenol blue), using the following programs: 10 h at 20 V, 30 min at 500 V, 30 min at 1000 V, and 4.5 h at 3000 V. Proteins were loaded onto a pair of identical pH 4–7 IPG strips in each experiment. After the first dimension, strips were cut into three fragments, each representing one pH unit. The pH 4–5 fragment was discarded because it did not contain pituitary autoantigens. The pH 5–6 and 6–7 fragments were then run on 4–12% SDS-PAGE for the second dimension. From the pair of identical strips, one gel set was stained by Coomassie blue and the other instead transferred to nitrocellulose membranes (GE Healthcare). These were blocked in PBS-3% BSA, and incubated overnight at 4 C with diluted sera (1:200) from CFA-only mice. Membranes were then washed and incubated for 1 h at room temperature with an antimouse IgG antibody, conjugated to horseradish peroxidase. Antibody binding was then detected using a chemiluminescent substrate (ECL; GE Healthcare). The membranes were then stripped, according to the manufacturer's recommendation (GE Healthcare), and probed with the immune sera. Images produced by immune sera were compared with those from CFA-only sera to identify unique protein spots. These spots were then matched to the gels stained by Coomassie blue, excised, in-gel digested with trypsin, and submitted for matrix-assisted laser desorption/ionization time-of-flight sequencing at the Proteomics Facility of the Johns Hopkins School of Medicine, as previously described (18).

Statistical analysis

The study was mainly designed to analyze cross-sectionally the pituitary infiltration score (the primary outcome) at multiple time points after immunization. This score was expressed as percentage (continuous scale from zero to 100) and calculated as follows: sum of the infiltrated areas in the anterior pituitary divided by the total anterior pituitary area times 100. The posterior and intermediate lobes were not included in the measurements because their mononuclear infiltration was rare and scanty. The pituitary of nonimmunized or CFA-only immunized mice contained only a few lymphocytes, representing about 0.5 $\pm$ 0.2% of the total area. Mice with an infiltration score greater than 2% were classified as EAH cases. Differences in the mean infiltration score were analyzed using a multiple linear regression model that included as covariates strain, sex, type of immunogen, dose of immunogen, and time after immunization. Differences in EAH cumulative incidence among strains were assessed by calculating the relative risks. Secondary outcomes were serum pituitary antibodies, T_4 and corticosterone, and the number of CD45 positive cells in the pituitary. Pituitary antibody values were first transformed to a logarithmic scale to approximate the normal distribution, and then analyzed by univariate regression using day after immunization as covariate and fractional polynomial fit. Corticosterone and T_4 were analyzed by univariate linear regression *vs.* day after immunization. The number of CD45 positive lymphocytes infiltrating the pituitary was compared among groups by the Wilcoxon rank sum test performed after the Kruskal-Wallis test.

Results

Female SJL/J mice are susceptible to EAH

Considering the known influence of the major histocompatibility complex locus (19) and sex (20) on autoimmune diseases, we tested 146 mice from six inbred strains of both sexes for their susceptibility to EAH upon pituitary whole extract immunization. SJL/J developed EAH with significantly higher incidence (relative risk = 23, 95% confidence interval (CI) 10–55; $P < 0.0001$) and greater severity [$P < 0.0001$] than the other five strains (Fig. 1A). Female SJL/J mice developed more severe EAH than male SJL/J mice ($P < 0.0001$; Fig. 1B), in keeping with the sex bias observed in patients with AH (1). Female FVB/N mice proved also susceptible to EAH (Fig. 1A), although with lower incidence (five of 10 mice) and milder severity (mean pituitary infiltration score = 6%, median = 3%). Based on these results,

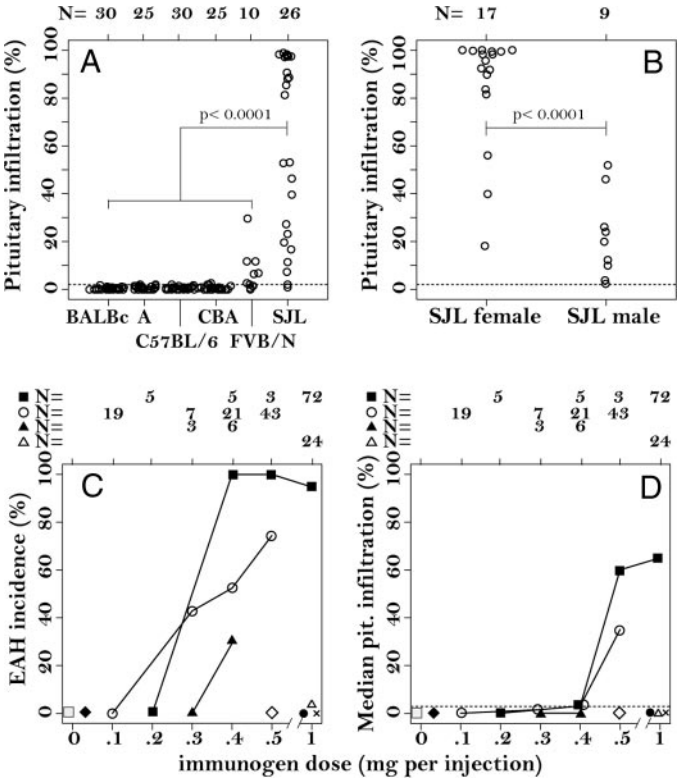

FIG. 1. Effect of strain, sex, immunogen type, and immunogen dose on EAH. A, SJL/L mice are susceptible to EAH. Six inbred strains, comprising a total of 146 mice, were analyzed for their susceptibility to EAH 28 d (±4) after immunization with mouse pituitary whole extract. B, Female preponderance. The pituitary lesions of the 26 SJL/J mice shown in panel A are now distributed according to sex, highlighting that females develop EAH with higher incidence and severity than males. C, EAH incidence in female SJL/J mice, according to immunogen type and dose. Mouse pituitary whole extract (*filled squares*, n = 85) and mouse pituitary cytosol (*open circles*, n = 90) were the strongest inducers of EAH. Mouse pituitary membrane (*filled triangles*, n = 9) and AtT-20 cells (*open triangles*, n = 24) also induce EAH but with low incidence. Pituitary nuclei (*open diamond*, n = 5), placental whole extract (*filled circle*, n = 15), and the other five pituitary cell lines (the *X symbol*, n = 25) do not induce EAH. The pituitary of these mice looked similar to that of mice immunized with CFA only (*filled diamond*, n = 7) or the nonimmunized controls (*open square*, n = 17). D, EAH severity in female SJL/J mice, according to immunogen type and dose. This graph shows the severity of EAH for the same 277 mice illustrated in panel C. In all panels, *the numbers above the panels* indicate the mouse number for each of the x-axis categories.

SJL/J females were used for all the other experiments presented in this paper.

The pituitary cytosolic fraction is enriched for autoantigen(s)

The mouse pituitary whole extract (*filled squares* in Fig. 1, C and D) induced EAH with the highest incidence and severity: incidence was more than 95% at doses more than or equal to 0.4 mg/injection (Fig. 1C); severity increased in a dose-dependent manner from 0% at 0.2 mg, 3% at 0.4 mg, to 60% at 0.5 mg, plateauing thereafter (65% at 1 mg, Fig. 1D). Pituitary cytosolic proteins (*open circles* in Fig. 1, C and D) were also reliable inducers of EAH: incidence and severity increased in a dose-dependent fashion, paralleling the trend seen with the whole extract. On the contrary, pituitary membranes (*filled triangles*) induced only a very mild disease (Fig. 1D) with low incidence (Fig. 1C), and pituitary nuclei (*open diamonds*) were ineffective. These results indicate that the pathogenic autoantigens of EAH mainly reside in the cytosolic compartment of the pituitary gland.

The mononuclear infiltration induced by pituitary immunization was seen only in the pituitary gland, and not in any of the thyroids and pancreata collected at the time mice were killed, even when using the highest dose of pituitary extract. In addition, control placental proteins (*filled circle* in Fig. 1, C and D) were incapable of inducing EAH, similar to what was observed in nonimmunized mice (*open square*) or CFA-only immunized mice (CFA controls, *filled diamond*). None of the six mouse pituitary cell lines was capable of inducing EAH with significant incidence or severity (Fig. 1, C and D).

The pathology of murine EAH closely resembles the human disease

After immunization with pituitary whole extract or cytosol, the pituitary gland developed a marked mononuclear cell infiltration of the anterior pituitary (Fig. 2, compare the pituitary of an immunized mouse in panel B with that of a CFA control pituitary in panel A). Infiltrating cells surrounded and destroyed the endocrine cells, ultimately effacing the normal acinar architecture (Fig. 2, compare panel D with panel C). The intermediate and posterior lobes were not involved with this immunization protocol. The mononuclear cells were mainly composed of CD3+ T cells (Fig. 3A) and B220+ B cells (Fig. 3B), which were present both diffusely throughout the gland and in focal collections. Other

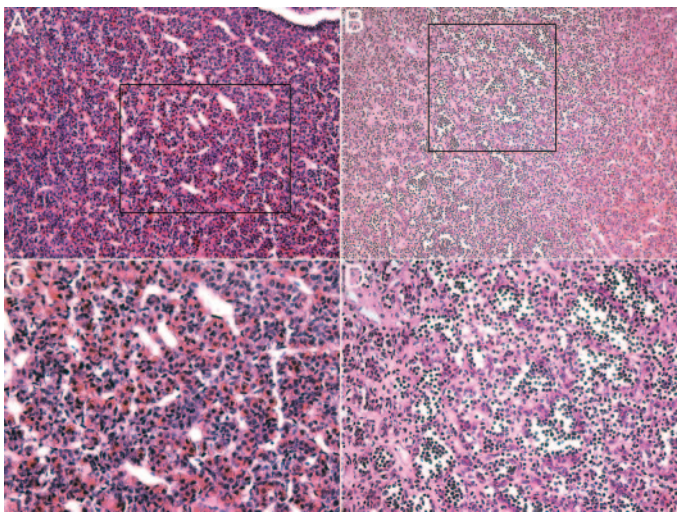

FIG. 2. EAH resembles the human disease. SJL/J female mice immunized with pituitary whole extract or pituitary cytosol develop a marked mononuclear cell infiltration of the pituitary gland that obliterates the normal pituitary architecture. A, Normal histology of the adenohypophysis from a d 28 CFA control mouse (magnification, ×20). B, Adenohypophysis from a d 28 mouse immunized with pituitary whole extract (magnification, ×20). C and D, Higher magnifications (×40) of the *boxed areas* in panels A and B. Note how in panels B and D the normal acinar structure is disrupted and replaced by the infiltrating mononuclear cells.

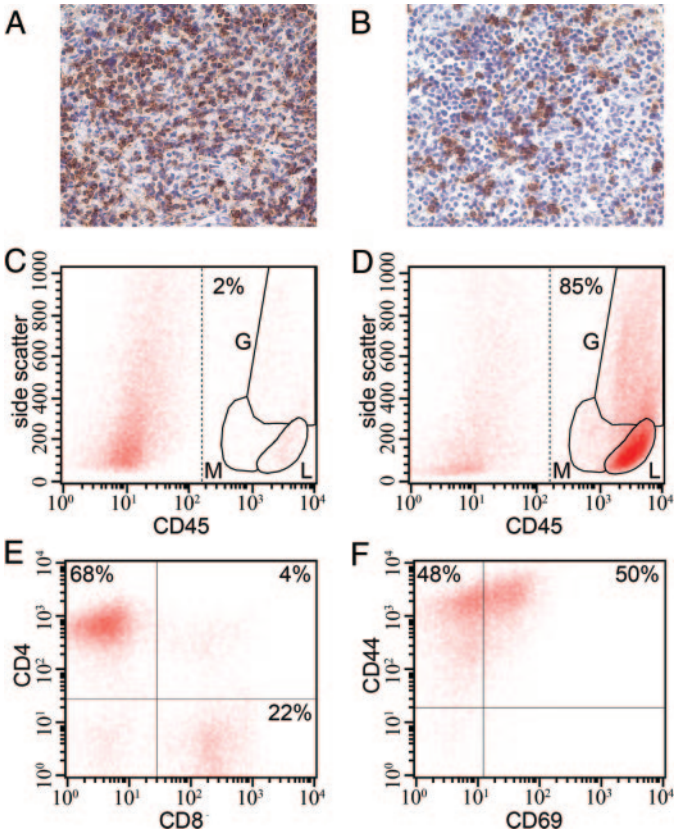

FIG. 3. T lymphocytes are the dominant cell type infiltrating the pituitary of SJL/J mice. A, Immunohistochemical analysis shows abundant CD3$^+$ T lymphocytes in the pituitary of mice immunized with pituitary whole extract. B, B220+ B lymphocytes are also present but less frequent. Flow cytometric analysis shows that CD45$^+$ hematopoietic cells represent only 2% of the total pituitary cells in normal pituitaries (C), but increase to 85% on d 28 after immunization (D). Lymphocytes (L gate) are the most abundant infiltrating population, although monocytes/macrophages (M gate) and granulocytes (G gate) can also be seen. E, Analysis of CD4 and CD8 coreceptors on CD3 gated cells show that CD4$^+$ T lymphocytes are 3-fold more abundant than CD8$^+$ T lymphocytes. F, The majority of CD4+ T lymphocytes express high levels of CD44, indicating an activated/memory phenotype.

cell types like granulocytes (compare the G gate in panels C and D of Fig. 3) and plasma cells (data not shown) also increased, although less abundantly, after immunization.

T cells show an activated/memory phenotype and are the key mediators of EAH

Flow cytometric analysis of the pituitary gland revealed that the percentage of CD45 positive hematopoietic cells increased from the normal 2% (Fig. 3C) to 85% (Fig. 3D) after immunization. Lymphocytes were the dominant population (L gate in Fig. 3D), representing 70% of the total CD45 positive cells. CD3 T cells were the most abundant lymphocytes (Fig. 3A), followed by B220 B cells (Fig. 3B), with average percentages of 78 and 10%, respectively (data not shown). CD4 T cells were about 3-fold more numerous than CD8 T cells (68 *vs.* 22%, Fig. 3E), highlighting the key role for CD4 T cells in disease pathogenesis. In fact, CD4 T cells are the first cells to enter a gland targeted by autoimmunity, triggering the development of tertiary lymphoid follicles (21), and are the most abundant T-cell subset in early disease phases (22, 23). The majority of CD4 cells showed an activated/memory phenotype, as indicated by homogeneously high levels of CD44 (Fig. 3F). CD69, an early T-cell activation marker, was also expressed at high levels on about 50% of the CD4 cells. A similar activation profile was displayed by CD8 cells (data not shown). The activated/memory phenotype of T cells is consistent with an ongoing inflammatory process within the pituitary gland. T cells were capable of transferring EAH to naive recipients upon adoptive transfer. All five recipients developed lymphocytic infiltration of the pituitary of mild severity (median infiltration score 5%, range 2–10%), whereas thyroids and pancreata were normal (data not shown).

Evolution of murine EAH: from pituitary expansion to atrophy

The natural history of human AH is poorly defined and variable, with outcomes ranging from complete remission through panhypopituitarism (1). We used our mouse EAH model induced by pituitary whole extract to elucidate how disease unfolds over time for extrapolating information to the human disease. Infiltration first appeared in the pituitary gland on d 14 after immunization and was characterized by small lymphoid infiltrates occupying about 5% of the gland (Fig. 4A, *arrow*). These initial infiltrates were mainly present within the sinusoidal spaces and did not disrupt the normal acinar architecture (data not shown). The disease then rapidly worsened by d 21 and 28, with infiltrating lymphocytes replacing about 50% of the anterior pituitary (Fig. 4A), and remained severe thereafter.

Further analysis of individual pituitary scores (Fig. 4B), rather than means as in Fig. 4A, revealed the existence of two modes of EAH early development. In the majority of female SJL/J mice, EAH developed very rapidly and severely (Fig. 4B, *open circles*). In the remainder, EAH was milder and progressed more slowly but still with a worsening trend (Fig. 4B, *filled diamonds*). The pituitary score differed on average by

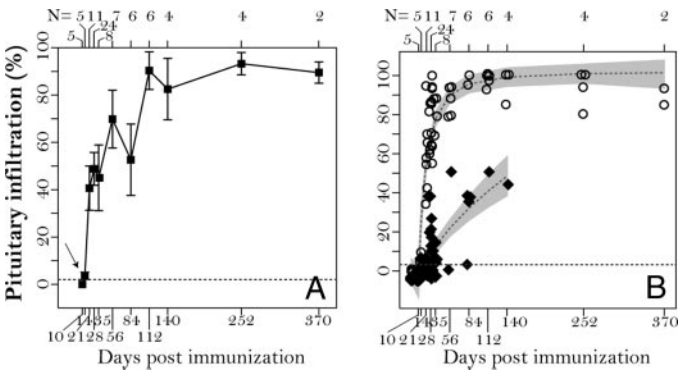

FIG. 4. Evolution of EAH in 82 female SJL/J mice immunized on d 0 and 7 with 1 mg pituitary whole extract. A, EAH severity in female SJL/J mice after pituitary whole extract immunization. Shown is the mean ± SE of the pituitary score at various time points after two immunizations. B, Fractional polynomial regression analysis reveals two modes of disease progression: fast responder (*open circles*) and slow responder (*filled diamonds*). *Shaded area* represents the 95% CIs for each group.

27% (95% confidence limits from 15–40%; $P < 0.0001$) between the fast and slow responders.

The pituitary gland on d 28 after immunization was markedly enlarged, inflamed, and firmly adherent to the surrounding meningeal structures (Fig. 5B, compare it with the normal pituitary of a CFA-only immunized control in Fig. 5A). With time, the pituitary gland markedly decreased in size as the tissue atrophied (Fig. 5C) such that it contained few adenohypophyseal cells by d 252 after immunization. The disease remained mainly lymphoid in nature throughout the entire course; by d 140 after immunization, lymphocytes could be seen in large aggregates (Fig. 5D). In addition, other pathological features appeared at later time points. Multinucleated giant cells (Fig. 5E) could be seen between d 35 and 84, which directly related to disease severity and resembled some of the lesions observed in patients with granulomatous hypophysitis. Fibrotic changes appeared as early as d 35 or 56, and became more prominent at later time points (Fig. 5F).

Pituitary antibodies predict hypophysitis severity in the florid phase of EAH

Pituitary antibodies increased rapidly after immunization, with a steep slope between d 0 and 21 (Fig. 6A), a period that we called the initiation phase. Pituitary antibodies did not correlate with disease severity at this time (Fig. 6B, *filled diamonds*) because pituitary disease is minimal during the initiation phase. Between d 21 and 140 after immunization, pituitary antibodies remained elevated and did not change significantly in titer (Fig. 6A). During this period, which we named the florid phase, antibody levels directly correlated with disease severity (Fig. 6B, *open squares*). The pituitary infiltration score increased on average 17% for every unit increase in the logarithm of the antibody AU (95% CI between 8 and 27%; $P = 0.001$). Beyond d 140, the atrophic phase, the pituitary antibody titers gradually declined, although remaining significantly higher than at baseline even 370 d after immunization (Fig. 6A), and did not correlate with EAH severity (Fig. 6B, *filled triangles*).

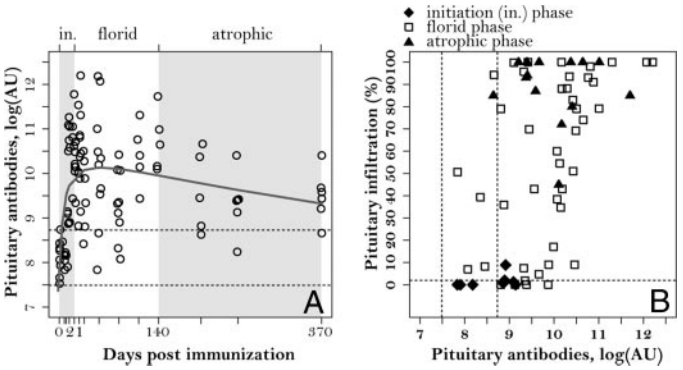

FIG. 6. Antibody levels, expressed as logarithms of AU, correlate with severity in the florid phase of EAH. A, Fractional polynomial regression analysis shows the overall antibody response (*solid line*) after immunization. The *dotted horizontal lines* represent the 5th to 95th percentile of pituitary antibody titers in preimmunized mice. B, Relation of pituitary infiltrating score and antibody titers, according to the different EAH phases. *Filled diamonds* represent pituitary antibodies in the initiation (in) phase (from d 0–14 after immunization), *open squares* in the florid phase (from d 21–140), and *filled triangles* in the atrophic phase (from d 140–370).

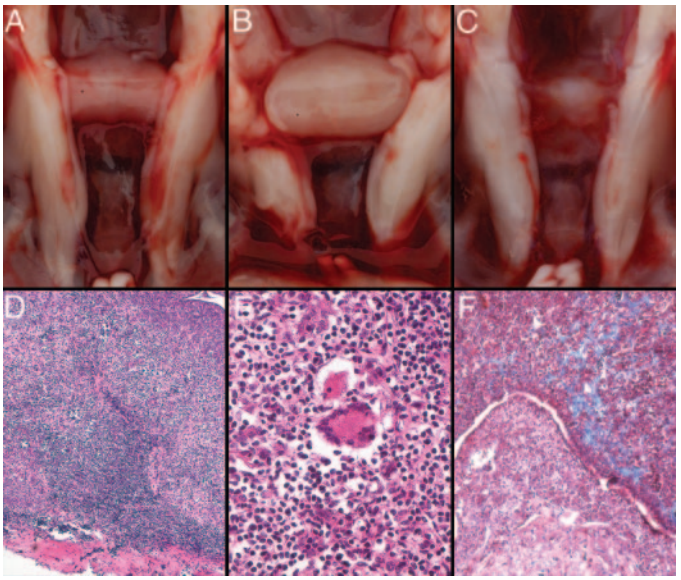

FIG. 5. Gross anatomical appearances of pituitaries from SJL/J mice immunized with CFA-only (A) or pituitary whole extract at d 28 (B) and d 252 (C) after immunization. D, Large collection of lymphoid cells can be seen in the pituitary at a late time point (140 d after immunization; ×40). E, Multiple nucleated giant cells appear between d 35 and 84 after immunization (×100). F, Fibrotic lesion (*light blue staining*; ×40).

Hypopituitarism is the common endpoint of EAH

We studied the function of the pituitary gland throughout the course of EAH by measuring the serum levels of corticosterone, T_4, and IGF-I. All hormones decreased with time (Fig. 7, A and B, and supplemental Fig. 1), indicating that hypopituitarism is the final outcome of the lymphocytic infiltration of the pituitary gland. However, corticosterone levels were more informative. They decreased below the normal range sooner than T_4 levels (d 56 in Fig. 7A *vs.* d 112 in Fig. 7B), suggesting that the ACTH-producing cells are an earlier or preferential target of the autoimmune response in the pituitary. They also showed in some of the mice a marked increase at d 28, possibly reflecting the host's attempt to control the autoimmune attack on the pituitary by increasing the output of ACTH and glucocorticoids. Indeed, mice with the highest corticosterone levels were generally the ones with the milder pathology (Fig. 7C, *open squares in the lower-right region*). By contrast, mice with the most severe EAH often had the lowest corticosterone levels (Fig. 7C, *open squares in the upper-left region*). All mice with atrophic pituitaries developed hypocortisolism (Fig. 7C, *filled triangles*). T_4 levels also showed an inverse correlation with pituitary pathology, with the lowest levels observed in mice with the most severe disease (Fig. 7D, *upper-left region*).

Novel autoantigens in EAH

The aforementioned described mouse model of AH was also developed with the goal of obtaining a tool that could aid in the discovery of pituitary autoantigen(s), which has thus far escaped identification. We used a proteomic ap-

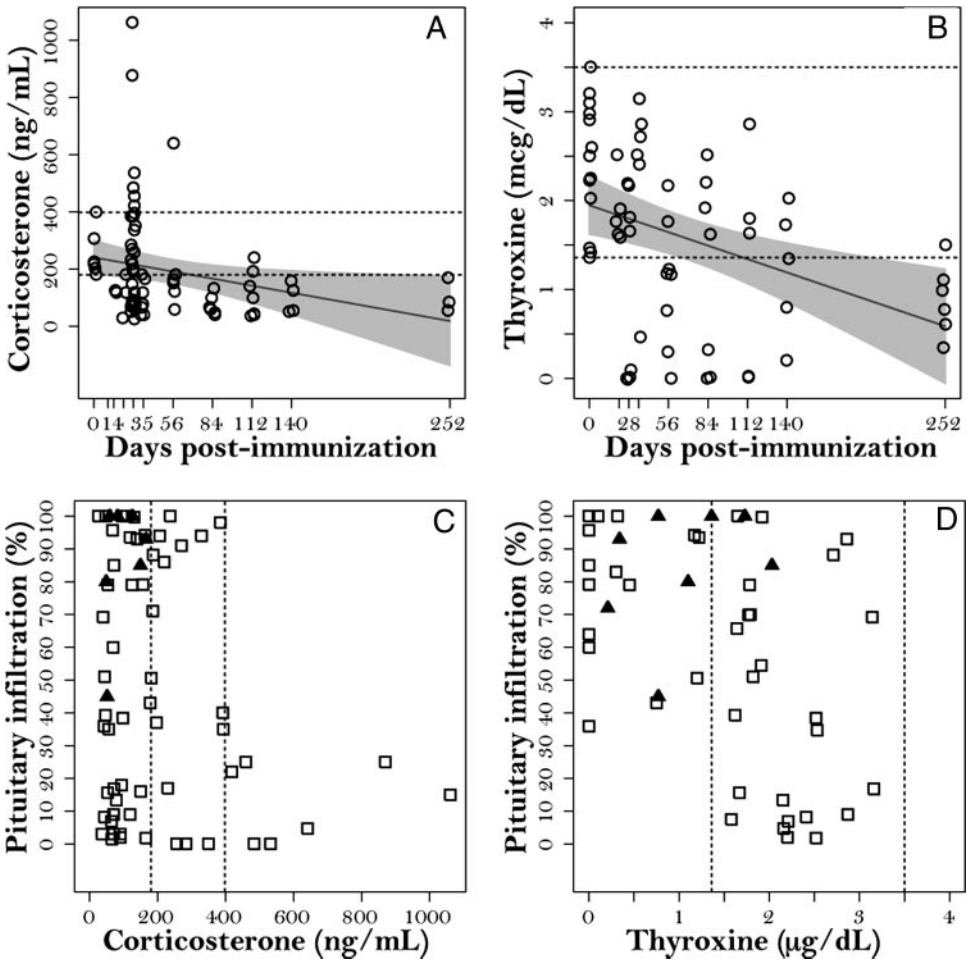

FIG. 7. Endocrine defects in immunized SJL/J mice. Simple linear regression analysis shows how corticosterone (A) and T_4 (B) levels change after immunization with pituitary whole extract. In both A and B, regression fit and 95% CI are represented by the *solid lines and shaded area*, respectively. The *dotted horizontal lines* indicate the 5th to 95th percentile of hormone levels in preimmunized mice. Correlation between pituitary infiltrating score and corticosterone (C) or T_4 (D) levels, according to EAH phases. *Open squares* represent hormone levels in the florid EAH phase (from d 21–140 after immunization), *filled triangles*, in the atrophic phase (d 140–370). The *dotted vertical lines* show the 5th to 95th percentile of hormone levels in preimmunized mice.

proach based on two-dimensional gel electrophoresis, immunoblotting comparison of immune *vs.* control sera, and protein sequencing by matrix-assisted laser desorption/ionization time-of-flight mass spectrometry of the protein spots recognized by the immune sera. Immune sera recognized eight unique spots from the pituitary cytosolic fraction (six of them shown in supplemental Fig. 2), and seven from the pituitary membrane fraction (data not shown). Sequencing yielded 62 (supplemental Table 1) and 56 (supplemental Table 2) candidate autoantigens, respectively. These 118 candidates need to be tested systematically for their ability to induce EAH in mice, and the autoantigens identified then tested against a range of human sera. However, some candidates, like sorting nexin 1 and PC2 in the cytosolic fraction and proopiomelanocortin and aminopeptidase B in the membrane fraction, are already attractive because of the high pituitary expression (24, 25), specific subcellular location (26, 27), and clinical notion that human corticotroph cells are the most frequently damaged cells in AH patients (28). We arbitrarily selected PC2 from the list of 118 candidate autoantigens as a tester to establish the system for mammalian expression and purification (supplemental Fig. 3). Upon immunization, PC2 induced a hematopoietic infiltration of the pituitary gland that was significantly greater than that seen in CFA-only immunized mice ($P = 0.0028$ by Wilcoxon rank sum test; supplemental Fig. 4A). However, EAH incidence and severity were low: seven of 20 mice (35%) developed an infiltration greater than 2% (supplemental Fig. 4A); and in only one mouse was the infiltration moderately severe (supplemental Fig. 4B). Nevertheless, the infiltration was pituitary specific and not seen in thyroids or pancreata (data not shown). Overall, these results suggest that PC2 is a minor pituitary autoantigen, and that additional autoantigens contribute to EAH initiation and progression.

Discussion

The study reports the first reliable mouse model of AH, induced by immunization of SJL/J female mice with mouse pituitary extract. Immunized mice developed a pituitary disease that closely mimicked the human counterpart. Pathologically, the disease was characterized by a diffuse lymphocytic infiltration of the anterior pituitary, comprising predominantly CD4+ T cells. Genetically, severe disease developed only in the SJL strain and the female sex, recapitulating the well-described impact of the major histocompatibility complex locus (29) and the less well-understood influence of sex (20) on autoimmune susceptibility. A few animal models of AH have been attempted since 1964 (14, 30–35), but induction of pituitary lymphocytic infiltration was scanty or not reproducible. The success of the present

mouse model probably derives from the use of a responsive strain and a suitable antigen dose (Fig. 1).

Several inferences about human AH have emerged from investigations of this new model. The pituitary gland was invariably enlarged in the early disease phase, consistent with the compression symptoms that may be identified in AH patients at presentation. It then gradually diminished in size, ultimately resulting in an atrophic gland. Although all immunized mice were of similar age and received the same immunogen, the pituitary disease progressed by two modes (slow and fast responders in Fig. 4), which may relate to the variable disease course described in human AH (1).

Autoantibodies are currently the main diagnostic tool for monitoring the immunological activity of autoimmune diseases, and can be used for prediction, diagnosis, and therapeutic decisions (36). Pituitary antibodies, however, are poorly characterized in human AH because the specific autoantigen(s) is unknown, so that it is most commonly measured by indirect immunofluorescence (37). We showed that pituitary antibodies, measured by the more sensitive ELISA technique, significantly correlated with disease severity during the florid phase of EAH, suggesting that they will be a valid clinical adjunct in the management of AH, especially once the autoantigen(s) is identified. Pituitary antibodies decreased over time, gradually declining from d 140 after immunization throughout the atrophic phase. These findings are consistent with the notion that pituitary antibodies decline when measured longitudinally in patients with hypopituitarism (38), and suggest that their absence in patients with empty sella syndrome (39) does not necessarily exclude AH as a cause of secondary empty sella.

Hypopituitarism is the characteristic endocrine feature of AH. It typically requires long-term hormone replacement and most commonly involves defects of ACTH secretion (28). Adrenal insufficiency was also the key endocrine abnormality observed in our mouse model, and preceded the appearance of hypothyroidism. Interestingly, serum corticosterone levels inversely correlated with pituitary infiltration scores during the florid phase of EAH, such that the surges predicted by the regression analysis on d 28 and 56 (Fig. 7) were followed by a decrease in pituitary infiltration. These results suggest that subjects capable of mounting a strong glucocorticoid response control the pituitary inflammation better. The correlation disappeared in the atrophic phase, probably related to a loss of ACTH output from the pituitary. Overall, these findings imply that glucocorticoids used to reduce pituitary swelling are chiefly effective only during the initial phases of AH. Hypopituitarism in EAH resulted from the destruction of endocrine cells by the lymphocytic infiltrate. However, it could also be explained by the presence of autoantibodies that bind and block the pituitary hormones, rendering them unable to stimulate their target cells. No obvious relationship, however, was observed between pituitary antibodies and corticosterone or T_4 levels.

Another clinical implication that emerged from our EAH studies is that about multinucleated giant cells. These cells are traditionally observed during granulomatous hypophysitis but can be occasionally seen in AH. Some scholars have proposed that the two pathological forms represent "a spectrum of disease, with purely lymphocytic hypophysitis being the predominant early lesion, and the granulomatous component being the later component of the same disease process" (40, 41). In our EAH studies, multinucleated giant cells were clearly observed but only during a relatively short time interval (from d 35–84 after immunization). They can be considered as a tissue response during a florid autoimmune attack, reflecting the macrophage clearance of pituitary cells damaged by the infiltrating lymphocytes. Because of their restricted temporal appearance, they might be missed in human specimens depending on the phase of AH. This possible common origin of granulomatous and lymphocytic hypophysitis could be addressed by an analysis of the antigenic profiles recognized in each disease.

Our quest to identify the causative autoantigen(s) in EAH led to the discovery of several pituitary proteins preferentially recognized by the immune sera. These proteins will require a methodical analysis to express them and screen them by immunization to select the dominant autoantigen(s). The mouse results will then need to be validated for the specific recognition by human AH sera.

In conclusion, our study highlights the key features of a new mouse model of AH that provides insights into the natural history of the human disease. The study also reports mouse pituitary autoantigens that could lead to the development of novel diagnostic biomarkers in humans.

Acknowledgments

We thank Drs. William Baldwin and Peter Burger (Department of Pathology, Johns Hopkins University, School of Medicine, Baltimore, MD), and Dr. Roberto Salvatori (Department of Medicine, Johns Hopkins University, School of Medicine) for their valuable suggestions throughout the course of the project and for revising the manuscript.

Received December 7, 2007. Accepted March 24, 2008.

Address all correspondence and requests for reprints to: Patrizio Caturegli, Department of Pathology, Johns Hopkins University, School of Medicine, Ross Building, Room 632, 720 Rutland Avenue, Baltimore, Maryland 21205. E-mail: pcat@jhmi.edu.

This work was supported in part by National Institutes of Health Grant DK 55670 (to P.C.).

References

1. **Caturegli P, Newschaffer C, Olivi A, Pomper MG, Burger PC, Rose NR** 2005 Autoimmune hypophysitis. Endocr Rev 26:599–614
2. **Freda PU, Post KD** 1999 Differential diagnosis of sellar masses. Endocrinol Metab Clin North Am 28:81–117
3. **Schneider HJ, Aimaretti G, Kreitschmann-Andermahr I, Stalla GK, Ghigo E** 2007 Hypopituitarism. Lancet 369:1461–1470
4. **Leung GK, Lopes MB, Thorner MO, Vance ML, Laws Jr ER** 2004 Primary hypophysitis: a single-center experience in 16 cases. J Neurosurg 101:262–271
5. **Blansfield JA, Beck KE, Tran K, Yang JC, Hughes MS, Kammula US, Royal RE, Topalian SL, Haworth LR, Levy C, Rosenberg SA, Sherry RM** 2005 Cytotoxic T-lymphocyte-associated antigen-4 blockage can induce autoimmune hypophysitis in patients with metastatic melanoma and renal cancer. J Immunother 28:593–598
6. **Yang JC, Hughes M, Kammula U, Royal R, Sherry RM, Topalian SL, Suri KB, Levy C, Allen T, Mavroukakis S, Lowy I, White DE, Rosenberg SA** 2007 Ipilimumab (anti-CTLA4 antibody) causes regression of metastatic renal cell cancer associated with enteritis and hypophysitis. J Immunother 30:825–830
7. **Ridruejo E, Christensen AF, Mando OG** 2006 Central hypothyroidism and hypophysitis during treatment of chronic hepatitis C with pegylated interferon α and ribavirin. Eur J Gastroenterol Hepatol 18:693–694
8. **Sakane N, Yoshida T, Yoshioka K, Umekawa T, Kondo M, Shimatsu A** 1995 Reversible hypopituitarism after interferonalfa therapy. Lancet 345:1305
9. **Takao T, Nanamiya W, Matsumoto R, Asaba K, Okabayashi T, Hashimoto K** 2001 Antipituitary antibodies in patients with lymphocytic hypophysitis. Horm Res 55:288–292
10. **O'Dwyer DT, Smith AI, Matthew ML, Andronicos NM, Ranson M, Rob-**

inson PJ, Crock PA 2002 Identification of the 49-kDa autoantigen associated with lymphocytic hypophysitis as α-enolase. J Clin Endocrinol Metab 87:752–757
11. **Tanaka S, Tatsumi KI, Kimura M, Takano T, Murakami Y, Takao T, Hashimoto K, Kato Y, Amino N** 2002 Detection of autoantibodies against the pituitary-specific proteins in patients with lymphocytic hypophysitis. Eur J Endocrinol 147:767–775
12. **Bensing S, Hulting AL, Hoog A, Ericson K, Kampe O** 2007 Lymphocytic hypophysitis: report of two biopsy-proven cases and one suspected case with pituitary autoantibodies. J Endocrinol Invest 30:153–162
13. **Onodera T, Toniolo A, Ray UR, Jenson AB, Knazek RA, Notkins AL** 1981 Virus-induced diabetes mellitus. XX. Polyendocrinopathy and autoimmunity. J Exp Med 153:1457–1473
14. **de Jersey J, Carmignac D, Barthlott T, Robinson I, Stockinger B** 2002 Activation of CD8 T cells by antigen expressed in the pituitary gland. J Immunol 169:6753–6759
15. **Lamango NS, Zhu X, Lindberg I** 1996 Purification and enzymatic characterization of recombinant prohormone convertase 2: stabilization of activity by 21 kDa 7B2. Arch Biochem Biophys 330:238–250
16. **Caturegli P, Rose NR, Kimura M, Kimura H, Tzou SC** 2003 Studies on murine thyroiditis: new insights from organ flow cytometry. Thyroid 13:419–426
17. **Kimura H, Kimura M, Tzou SC, Chen YC, Suzuki K, Rose NR, Caturegli P** 2005 Expression of class II major histocompatibility complex molecules on thyrocytes does not cause spontaneous thyroiditis but mildly increases its severity after immunization. Endocrinology 146:1154–1162
18. **Colquhoun DR, Schwab KJ, Cole RN, Halden RU** 2006 Detection of norovirus capsid protein in authentic standards and in stool extracts by matrix-assisted laser desorption ionization and nanospray mass spectrometry. Appl Environ Microbiol 72:2749–2755
19. **Vladutiu AO, Rose NR** 1971 Autoimmune murine thyroiditis relation to histocompatibility (H-2) type. Science 174:1137–1139
20. **Whitacre CC** 2001 Sex differences in autoimmune disease. Nat Immunol 2:777–780
21. **Marinkovic T, Garin A, Yokota Y, Fu YX, Ruddle NH, Furtado GC, Lira SA** 2006 Interaction of mature CD3+CD4+ T cells with dendritic cells triggers the development of tertiary lymphoid structures in the thyroid. J Clin Invest 116:2622–2632
22. **Kohm AP, Carpentier PA, Anger HA, Miller SD** 2002 Cutting edge: CD4+CD25+ regulatory T cells suppress antigen-specific autoreactive immune responses and central nervous system inflammation during active experimental autoimmune encephalomyelitis. J Immunol 169:4712–4716
23. **Ng HP, Banga JP, Kung AW** 2004 Development of a murine model of autoimmune thyroiditis induced with homologous mouse thyroid peroxidase. Endocrinology 145:809–816
24. **Low MJ, Liu B, Hammer GD, Rubinstein M, Allen RG** 1993 Post-translational processing of proopiomelanocortin (POMC) in mouse pituitary melanotroph tumors induced by a POMC-simian virus 40 large T antigen transgene. J Biol Chem 268:24967–24975
25. **Marcinkiewicz M, Day R, Seidah NG, Chretien M** 1993 Ontogeny of the prohormone convertases PC1 and PC2 in the mouse hypophysis and their colocalization with corticotropin and α-melanotropin. Proc Natl Acad Sci USA 90:4922–4926
26. **Lindberg I, Ahn SC, Breslin MB** 1994 Cellular distributions of the prohormone processing enzymes PC1 and PC2. Mol Cell Neurosci 5:614–622
27. **Sauter NP, Toni R, McLaughlin CD, Dyess EM, Kritzman J, Lechan RM** 1990 Isolated adrenocorticotropin deficiency associated with an autoantibody to a corticotroph antigen that is not adrenocorticotropin or other proopiomelanocortin-derived peptides. J Clin Endocrinol Metab 70:1391–1397
28. **Caturegli P** 2007 Autoimmune hypophysitis: an underestimated disease in search of its autoantigen(s). J Clin Endocrinol Metab 92:2038–2040
29. **McDevitt HO** 1998 The role of MHC class II molecules in susceptibility and resistance to autoimmunity. Curr Opin Immunol 10:677–681
30. **Beutner EH, Djanian A, Witebsky E** 1964 Serological studies on rabbit antibodies to the rabbit anterior pituitary. Immunology 7:172–181
31. **Klein I, Kraus KE, Martines AJ, Weber S** 1982 Evidence for cellular mediated immunity in an animal model of autoimmune pituitary disease. Endocr Res Commun 9:145–153
32. **Lee HS** 1977 A serologic and histopathologic study of the adenohypophysis in rats immunized with extracts of isologous rat anterior pituitary in Freund's adjuvant and pertussis toxin. Seoul J Med 18:184–194
33. **Levine S** 1969 Allergic adrenalitis and adenohypophysitis: further observations on production and passive transfer. Endocrinology 84:469–475
34. **Watanabe K, Tada H, Shimaoka Y, Hidaka Y, Tatsumi K, Izumi Y, Amino N** 2001 Characteristics of experimental autoimmune hypophysitis in rats: major antigens are growth hormone, thyrotropin, and luteinizing hormone in this model. Autoimmunity 33:265–274
35. **Yoon JW, Choi DS, Liang HC, Baek HS, Ko IY, Jun HS, Gillam S** 1992 Induction of an organ-specific autoimmune disease, lymphocytic hypophysitis, in hamsters by recombinant rubella virus glycoprotein and prevention of disease by neonatal thymectomy. J Virol 66:1210–1214
36. **Achenbach P, Bonifacio E, Koczwara K, Ziegler AG** 2005 Natural history of type 1 diabetes. Diabetes 54(Suppl 2):S25–S31
37. **Manetti L, Lupi I, Morselli LL, Albertini S, Cosottini M, Grasso L, Genovesi M, Pinna G, Mariotti S, Bogazzi F, Bartalena L, Martino E** 2007 Prevalence and functional significance of antipituitary antibodies in patients with autoimmune and non-autoimmune thyroid diseases. J Clin Endocrinol Metab 92:2176–2181
38. **Kajita K, Yasuda K, Yamakita N, Murai T, Matsuda M, Morita H, Mori A, Murayama M, Tanahashi S, Sugiura M** 1991 Anti-pituitary antibodies in patients with hypopituitarism and their families: longitudinal observation. Endocrinol Jpn 38:121–129
39. **Bensing S, Rorsman F, Crock P, Sanjeevi C, Ericson K, Kampe O, Brismar K, Hulting AL** 2004 No evidence for autoimmunity as a major cause of the empty sella syndrome. Exp Clin Endocrinol Diabetes 112:231–235
40. **McKeel DW** 1983 Common histopathological and ultrastructural features in granulomatous and lymphoid adenohypophysitis. Endocrinology 112:190 (Abstract 437)
41. **McKeel DW** 1984 Primary hypothyroidism and hypopituitarism in a young woman: pathological discussion. Am J Med 77:326–329
42. **Shen FS, Seidah NG, Lindberg I** 1993 Biosynthesis of the prohormone convertase PC2 in Chinese hamster ovary cells and in rat insulinoma cells. J Biol Chem 268:24910–24915

***Endocrinology* is published monthly by The Endocrine Society (http://www.endo-society.org), the foremost professional society serving the endocrine community.**